

Protein folding using contact maps

Michele Vendruscolo and Eytan Domany

Department of Physics of Complex Systems, Weizmann Institute of Science, Rehovot 76100, Israel

Contents

I	Introduction	1
II	Structure representation	2
III	The reconstruction procedure	3
	A Growth	4
	B Adaptation	5
	C Results	6
	1 Experimental contact maps.	6
	2 Non-physical contact maps	7
IV	Dynamics in contact map space	8
	A Non-local dynamics	9
	B Local dynamics	11
	C Reconstruction	11
	D Refinement:	12
V	An approximation for the free energy	14
	A The (free) energy associated with a contact map	14
	B Optimization	15
	C Learning the energy parameters by a perceptron	15
VI	Results	17
	A Threading	18
	B Crambin	21
	1 Learning the pairwise contact term	22
	2 Energies of the false ground states	22
	3 Learning the hydrophobic term	24
	C Immunoglobulins	24
	1 Learning the pairwise contact term	25
	2 Learning the hydrophobic term	25
VII	Final considerations	26

I. INTRODUCTION

Computational approaches to protein folding are divided into two main categories. In *energy minimization* methods the native state is identified with the the ground state of a suitable energy function (Brooks, 1998). In *fold recognition* methods, the native state is selected as the most compatible structure among those present in a library (Bowie *et al.*, 1992; Jones *et al.*, 1992; Fisher *et al.*, 1996). Both approaches depend on three important choices: 1) The representation of protein structure; 2) The set of alternative structures among which the native fold is sought for; 3) A bias towards the “best” conformation. In energy minimization approaches such a bias is an energy function, and the best conformation is the one of lowest energy. On the

other hand, in fold recognition methods, a compatibility function for a sequence on a structure is used. The compatibility is often expressed in terms of database-derived properties and restraints.

In this review we analyze the attempt to use contact maps to efficiently perform protein fold prediction. Contact maps are a particularly manageable representation of protein structure which has been already applied in the past to the study of protein conformation (Chan and Dill, 1990), structure comparison (Holm and Sander, 1993), interaction patterns in proteins (Lifson and Sander, 1979; Godzik *et al.*, 1993) and correlated mutations (Olmea and Valencia, 1997; Ortiz *et al.*, 1998). The possibility of performing energy minimization in the space of contact maps has been proposed by Mirny and Domany (1996). We present here the consistent development of their idea, discussing successes, failures and perspectives.

II. STRUCTURE REPRESENTATION

We discuss the problem of representations of protein structure and give the definition of contact maps.

Following Anfinsen’s thermodynamic hypothesis (Anfinsen, 1973), the native state of a protein is commonly assumed to be the minimum of a free energy function. This is a powerful assumption and Molecular Dynamics is the most direct method to implement it (Brooks, 1998). The structure is represented by listing the coordinates of all the atoms and Newton’s equation of motion are solved in a suitable force field tuned for molecular systems. Unfortunately, present computers cannot follow the trajectory of a protein all the way down to its native state. The best result to date is the simulation of 1 μ s trajectory of villin headpiece subdomain in water which allowed the detection of the hydrophobic collapse and of the formation of secondary structures (Duan and Kollman, 1998). Furthermore, the method depends crucially on the determination of suitable energy parameters. An incorrect energy function, which does not assign the lowest energy to the native conformation, leads a careful energy minimization procedure to some misfolded conformation, as for example shown by Karplus and collaborators in the case of hemerythrin and the immunoglobulin VL domain (Novotny *et al.*, 1984).

We believe that perhaps one can solve the problem without going to such microscopic detail and we set about to investigate this assumption. The problem of structure representation is to find the best trade-off between computability and accuracy of the predictions. Our inclination is that good predictions can be obtained by constructing simplified models.

Lattice models offer the possibility to gradually turning on the complexity of the representation of the structure. Usually a protein is represented as a chain of monomers occupying lattice sites and representing C_α atoms. The complexity can be measured by the number of states available to each monomer (Park and Levitt, 1995). The lowest possible complexity is that of tetrahedral and simple cubic lattices, where 3 and 5 states per monomer are respectively available. Lattices of high coordination number, up to 55 states, have been studied (Ortiz *et al.*, 1998). The main motivation to study lattice models is that at low complexity it is possible to effectively solve the problem of searching the ground state, either exactly, by enumerating all the conformations or approximately, by Monte Carlo methods. By using Monte Carlo simulations, solutions can be routinely obtained for polymers up to length 125 (Šali *et al.*, 1994; Dinner *et al.*, 1996). Using pairwise contact energy functions, evidence for important features of the folding process has been produced, most notably, the hydrophobic collapse. It is possible to consider more detailed lattice models which still retain some of the advantage in computability and allow a more realistic representation of protein structure: for example, it is possible to represent side chains by an additional virtual atom. Advances in this direction have been recently reported by Skolnick and collaborators (Ortiz *et al.*, 1998). Interestingly, the accuracy increases very slowly with the complexity, and the typical resolution of structures in the Protein Data Bank (PDB) (Bernstein *et al.*, 1977) can be obtained with models with 10 to 20 states (Park and Levitt, 1995). The C_α model can be simulated also off-lattice. For short chains and simple interactions it is possible to identify the ground state with reasonable reliability (Clementi *et al.*, 1998; Irbäck and Potthast, 1995).

A minimalistic representation of a protein’s structure is given by its *contact map* (Lifson and Sander, 1979; Chan and Dill, 1990; Godzik *et al.*, 1993; Hold and Sander, 1993; Mirny and Domany, 1996; Vendruscolo *et al.*, 1997). The contact map of a protein with N residues is an $N \times N$ matrix \mathbf{S} , whose elements are defined as

$$S_{ij} = \begin{cases} 1 & \text{if residues } i \text{ and } j \text{ are in contact} \\ 0 & \text{otherwise} \end{cases} \quad (1)$$

One can define contact between two residues in different ways; one is to consider two amino acids in contact when their two C_α atoms are closer than some threshold R_c (“ C_α ” definition) (Vendruscolo *et al.*, 1997). Another definition is based on the minimal distance between two atoms that belong to the two residues (Hinds and Levitt, 1994; Mirny and Domany, 1996) (“all atoms” definition). In a contact map α -helices appear as thick bands of contacts along the diagonal, β -sheets as bands running parallel or perpendicular to the diagonal. Given all the inter-residue contacts or even a subset of them, it is possible to reconstruct quite well a protein’s structure, by means of either Distance Geometry (Crippen and Havel, 1988), Molecular Dynamics (Brünger *et al.*, 1986) or Monte Carlo (Vendruscolo *et al.*, 1997).

In contrast to Cartesian coordinates, the map representation of protein structure is independent of the coordinate frame. This property made contact maps attractive for protein structure comparisons and for *searching a limited database* for similar structures (Chan and Dill, 1990; Godzik *et al.*, 1993; Hold and Sander, 1993).

One of the main reasons for selecting the contact map representation of structure is our expectation and hope that we may be able to search the space of contact maps in an efficient manner and find low energy maps (that hopefully correspond to conformations close to the native one). In particular, one hopes that relatively simple changes on a map may generate very substantial coherent moves of the corresponding polypeptide chain conformation; moves which would have taken much longer to achieve by working with the chain itself.

In order to actually implement such moves in the space of contact maps, one has to overcome two important problems. The main and foremost one is the need to ensure that the map \mathbf{S} that has been generated is *physical*. Our definition of “physical” will be given in detail below; broadly speaking, we mean that there exists a chain conformation whose contact map is indeed our proposed \mathbf{S} . Arbitrary changes performed on a map yield, with very high probability, non-physical maps. The reason is that the total number of possible $N \times N$ contact maps is $O(2^{aN^2})$, whereas the number of physical maps is much smaller, of order $O(2^{bN})$. The need for a procedure that limits the search to the small subspace of physical maps was identified by Mirny and Domany (1996), who proposed a restricted set of moves. The hope was that when moves selected from this set are performed on a physical map, the new map is also physical. These rules were, however, heuristic and no clear proof of the validity of this hope could be given.

Subsequently, the problem of generating physical maps was dealt with by means of a *reconstruction procedure* (Vendruscolo *et al.*, 1997). For any proposed contact map \mathbf{S} one generates a chain, with \mathbf{S} serving as the guide of the construction process. The procedure stops when the contact map \mathbf{S}' of the resulting chain is close to the target map; this way one generates a map which is physical *and* close to the target.

The second important issue is the manner in which low energy maps are generated from an existing one (Vendruscolo and Domany, 1998a). The procedure has to be such that the resulting map is “protein-like”, i.e. has secondary structure elements and the corresponding chain has the right density, bond-angle distribution, chirality, etc. The final map should be physical and the decorrelation time with the starting map should be short.

In what follows we sketch how these two problems were addressed; for a more detailed description of these procedures the reader is referred to the original publications (Vendruscolo *et al.*, 1997; Vendruscolo and Domany, 1998a).

III. THE RECONSTRUCTION PROCEDURE

We present a method to obtain a three dimensional polypeptide conformation from a contact map. We also explain how to deal with the case of non physical contact maps.

The aim is to find an efficient procedure, which can be performed “on line” and in parallel with the dynamics in the space of contact maps, which will “project” any map onto a nearby one which is guaranteed to be physically realizable. The protein is represented as a “string of beads”, in which each bead stands for an amino acid - the coordinates of center of a bead are identified with those of the corresponding C_α

atom. For a given target contact map \mathbf{S} , the algorithm searches for a conformation that this string of beads can take, such that the contact map \mathbf{S}' of our string is similar (or close) to \mathbf{S} . If there exists a chain conformation whose contact map is identical with \mathbf{S} , this contact map is, by definition, physical. In general, our method aims at converting a possibly ill-defined, non-physical set of contacts to a legitimate one. The three dimensional structure is in our case a means, rather than the end.

It should be noted that related, previously developed methods (Havel *et al.*, 1979; Brünger *et al.*, 1986; Bohr *et al.*, 1993; Nilges, 1995; Lund *et al.*, 1996; Aszodi and Taylor, 1996; Mumenthaler and Brown, 1996; Skolnick *et al.*, 1997) a different aim; to construct three dimensional structures from measured distance information, using various forms of distance geometry (Crippen and Havel, 1988), supplemented by restricted Molecular Dynamics (Scheek *et al.*, 1989) or simulated annealing (Brünger *et al.*, 1997).

One should emphasize here the distinction between a contact map and a distance map. In a contact map a minimal amount of information is available - given a pair of amino acids, we know only if they are in contact or not. That is, only lower and upper bounds on their separation are given. A distance matrix, on the other hand, presents real-valued distances between pairs of amino acids. The method presented here is not restricted to contact maps and has been generalized to distance maps (Vendruscolo and Domany, unpublished). The deviations between different structures that were reconstructed from the same contact map are typically much higher than those between two structures derived from a distance matrix.

The proposed algorithm is divided into two parts. The first part, *growth*, consists of adding one monomer at a time, i.e. a step by step growth of the chain. The second part, *adaptation*, is a refinement of the structure, obtained as a result of the growth stage, by local moves. In both stages, to bias the dynamics, we introduce cost functions defined on the basis of the contact map. Such cost functions contain only geometric constraints, and do not resemble the true energetics of the polypeptide chain.

A. Growth

The first element of the growth is *single monomer addition*., which is carried out in the spirit of the Rosenbluth method (Rosenbluth and Rosenbluth, 1955). To add monomer i to the growing chain we generate at random N_t trial positions, (typically $N_t = 10$),

$$\mathbf{r}_i^{(j)} = \mathbf{r}_{i-1} + \mathbf{r}^{(j)}, \quad (2)$$

where $j = 1, \dots, N_t$. The length and the directions of $\mathbf{r}^{(j)}$ are set from a statistical analysis of PDB. One out of the N_t trials is chosen according to the probability

$$p^{(j)} = \frac{e^{-E_g^{(j)}/T_g}}{\sum_{j=1}^{N_t} e^{-E_g^{(j)}/T_g}}, \quad (3)$$

where E_g is a cost function which rewards contacts that should be present, according to the given contact map, and discourage contacts that should not be there.

The second element of the procedure is *chain growth*. The step by step growth just discussed optimizes the position of successive amino acids along the sequence. The main difficulty in the method is that the single step of the growing chain has no information on the contacts that should be realized many steps (or monomers) ahead. To solve this problem, we carry out several attempts (typically 10) to reconstruct the structure, choosing the best one. In practice, this is done as follows.

For each attempt, when position $\mathbf{r}^{[j(i)]}$ is chosen for monomer i according to Eq. (3), its probability is accumulated in the weight

$$W_i = \prod_{k=1}^i p_k^{[j(k)]} \quad (4)$$

When we have reached the end of the chain we store the weight W_N . The trial chain with the highest W_N is chosen.

The *cost function* for growth is

$$E_g^{(j)} = \sum_{k=1}^{i-1} d \cdot a_g(S_{ik}) \cdot \vartheta(d_t - r_{ik}^{(j)}) , \quad (5)$$

where $r_{ik}^{(j)} = |\mathbf{r}_i^{(j)} - \mathbf{r}_k|$. The enhancing factor $d = i - k$ is introduced to guide the growth towards contacts that are long ranged along the chain; ϑ is the Heaviside step function and the constant a_g can take two values; $a_g(S_{ik} = 0) \geq 0$ and $a_g(S_{ik} = 1) \leq 0$. That is, when a contact is identified in the chain, i.e. $r_{ik} < d_t$, it is either rewarded (when the target map has a contact between i and k), or penalized.

B. Adaptation

When we have grown the entire chain of N points, we refine the structure according to the following scheme. We choose a point i at random and try, using a crankshaft move (Šali *et al.*, 1994), to displace it to \mathbf{r}'_i , keeping fixed the distances from both points $i - 1$ and $i + 1$. We use a local cost function $E_a^{(i)}$:

$$E_a^{(i)} = \sum_{k=1}^N f_a(r'_{ik}) = a_a(S_{ik}) \cdot \vartheta(d_t - r'_{ik}) , \quad (6)$$

where $r'_{ik} = |\mathbf{r}'_i - \mathbf{r}_k|$. Note that the enhancing factor d has been omitted, so that f_a does not favor contacts between monomers that are distant along the chain. The displacement is accepted with probability π , according to the standard Metropolis prescription

$$\pi = \min(1, \exp(-\Delta E_a/T_a)) \quad (7)$$

where ΔE_a is the change in the cost function E_a induced by the move and T_a is a temperature-like parameter, used to control the acceptance ratio of the adaptation scheme.

A key ingredient of our method is annealing (Kirkpatrick *et al.*, 1983). As in all annealing procedures, the temperature-like parameter T_a is decreased slowly during the simulation to help the system find the ground state in a rugged energy landscape. In our method, however, instead of using simulation time as a control parameter on the temperature, we chose the number n of missing contacts. Two regimes were roughly distinguished. In the first regime many contacts are missed and the map is very different from the target one. In the second regime few contacts are missed, and the map is close to the target. The parameters a_a and T_a are interpolated smoothly between values suitable for these two limiting cases. In the first regime, we strongly favor the recovery of contacts that should be realized, whereas in the second regime we strongly disfavor contacts that are realized but should not be present. We set, as shown in Fig. 1

$$a_a^{(n)}(S) = a^f(S) + [a^i(S) - a^f(S)]\sigma(n) , \quad (8)$$

and

$$T_a^{(n)} = T_a^f + (T_a^i - T_a^f)\sigma(n) . \quad (9)$$

The function $\sigma(n)$ interpolates between the initial value a^i and the final value a^f ,

$$\sigma(n) = \frac{2}{1 + e^{-\alpha_g n}} - 1 . \quad (10)$$

By choosing a^i , a^f , T_a^i , T_a^f and α_g we define the two regimes, far from and close to the target map.

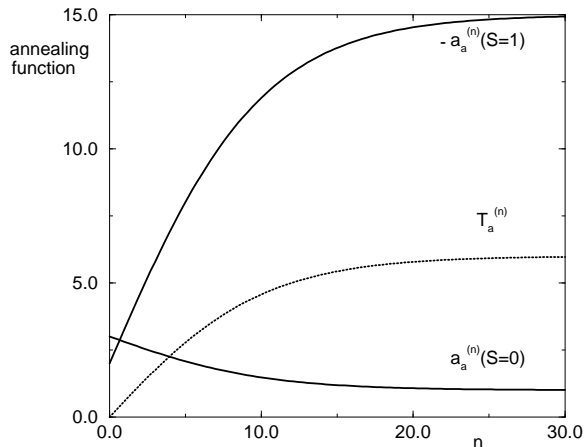


FIG. 1. Annealing functions for the parameters used in adaptation. See Eqs. (8) and (9).

We have tried several alternatives to each of the components of the method outlined above. For a detailed description of these, we refer the reader to Vendruscolo *et al.* (1997). We present here a brief description of some selected results that were obtained using the algorithm presented above.

C. Results

1. Experimental contact maps.

In this section we present results about the reconstruction of experimental contact maps as taken from PDB. Since our purpose, as explained in the Introduction, is to use the reconstruction in connection with dynamics, we chose the contact length $R_c = 9 \text{ \AA}$ to obtain the most faithful representation of the energy of the protein (Mirny and Domany, 1996). Such a threshold is determined by the requirement that the average number of $C_\alpha - C_\alpha$ contacts for each amino acid is roughly equal to the respective numbers obtained with the all-atom definition of contacts.

The most commonly used dissimilarity measure between structures is the root mean square (RMS) distance D (McLachlan, 1979)

$$D = \sqrt{\frac{1}{N} \sum_{i=1}^N (\mathbf{r}_i - \mathbf{r}'_i)^2}, \quad (11)$$

where one structure is translated and rotated to get a minimal D .

The dissimilarity measure between contact maps is defined as the Hamming distance

$$D^{\text{map}} = \sum_{j>i} |S_{ij} - S'_{ij}|, \quad (12)$$

which counts the number of mismatches between maps \mathbf{S} and \mathbf{S}' .

We present in Fig. 2a the results over 100 reconstruction runs for chains for the protein 6pti (bovine pancreatic trypsin inhibitor).

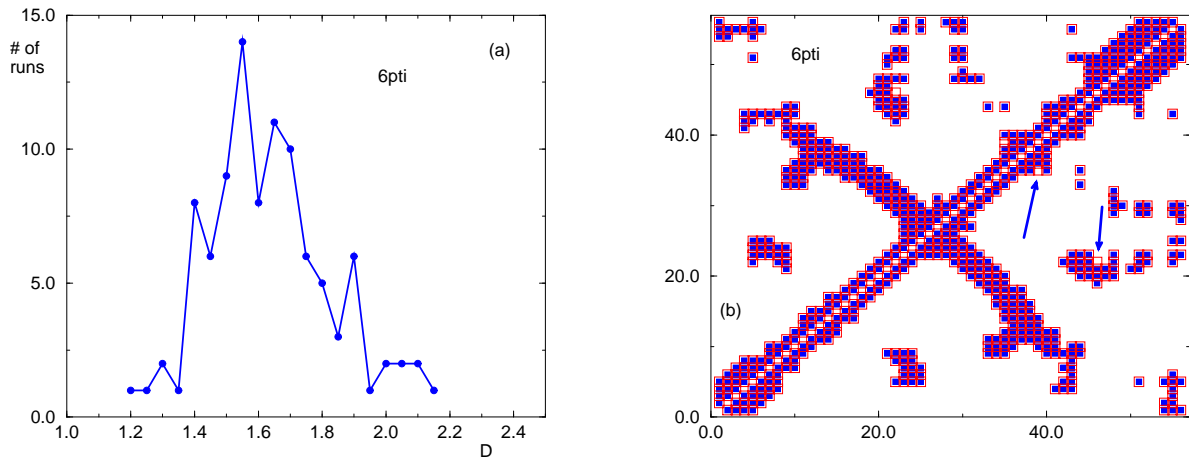


FIG. 2. (a) Histogram of the distance D for the 100 runs used to test the reconstruction procedure. Data are presented for protein 6pti. (b) Contact maps for protein 6pti for a threshold $d_t = 9 \text{ \AA}$. Full squares are the PDB data, open squares the output of the reconstruction procedure. None of the target contacts is missed and two spurious ones are added (the arrows point at their locations). (Adapted with permission from Vendruscolo *et al.* (1997). Copyright 1997 Current Biology.)

In Fig. 2b we show the contact map for the protein 6pti, $N = 56$, as taken from PDB, that was used as a target to construct a chain. The contact map of a typical reconstructed chain is also shown. In this particular case none of the 342 original contacts were missed and only two false positive contacts were added. These are close to clusters of correct contacts, indicating slight local differences with the crystallographic structure. The distance recorded in this case was $D = 1.56$.

We carried out extensive similar tests for other proteins of various lengths (Vendruscolo *et al.*, 1997). Our method produces, using a native contact map as target, a structure whose contact map is in nearly perfect agreement with the target. Furthermore, the distance of this reconstructed chain from the native structure is quite close to the resolution that can be obtained from the information contained in contact maps.

2. Non-physical contact maps

Our main purpose is to develop a strategy to construct a three dimensional structure, starting from a given set of contacts, even if these contacts are not physical, i.e. not compatible with any conformation allowed by a chain's topology. In such a case we require our procedure to yield a chain whose conformation is as "close" as possible to the contact map we started with. The exact measure of such closeness depends on the source of non-physicality, as will be demonstrated in two examples described below.

Our first examples of non-physical contact maps were obtained by randomizing a native contact map; this was done by flipping M randomly chosen entries. Contacts between consecutive amino acids (neighbors along the chain) were conserved.

A typical contact map with noise is shown in Fig. 3. The protein is 1trm chain A, whose contact map has 1595 contacts, when the threshold is set to 9 \AA . We show the native map and the target map obtained by flipping at random $M = 400$ entries of the native map, together with the map produced by our method. For the particular case shown, the distance to the crystallographic structure $D = 2.4 \text{ \AA}$.

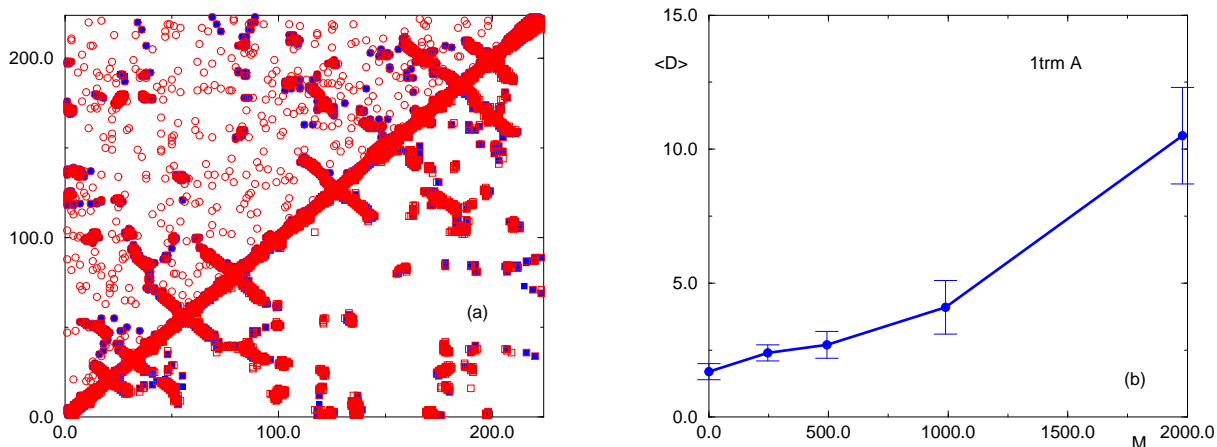


FIG. 3. (a) Above diagonal: reference map (open circles) obtained by randomizing the underlying physical map (full squares) of protein 1trm chain A. Below diagonal: reconstructed contact map (open square) obtained using the noise-corrupted map as target. (b) Average distances $\langle D \rangle$ versus noise M for protein 1trm A. (Adapted with permission from Vendruscolo *et al.* (1997). Copyright 1997 Current Biology.)

The most important conclusion that can be drawn from Fig. 3 is that isolated non-physical contacts are identified as such and ignored and the underlying physical contact map is recovered.

The dependence of this recovery on the noise level is shown in Fig. 3, where we present the average distance of the final structure from the uncorrupted 1trm A contact map, for various values of M . Averages were taken over 10 different realizations of the noise, and over 10 reconstruction runs for each realization. The distance for totally unrelated structures for 1trm A is around 15 Å. It is remarkable that up to $M < 1000$ a fair resemblance to the experimental structure is still found. Even with the addition of a noise which is around 60% of the signal, the reconstruction procedure works. We have found similar result for the smaller protein 6pti, which has 342 contacts, and can be fairly well reconstructed with a noise of up to 200 flipped contacts.

To summarize this section, for physically realizable target contact maps our method is very fast and reliable to find a chain conformation whose contact map is nearly identical to the target. Moreover, the method is able to find a good candidate structure even when the target map has been corrupted with non-physical contacts. The information contained in a known native contact map suffices to reconstruct a conformation, which is relatively close to that of the original structure, as was already observed by Havel *et al* (1979). There is, however, an intrinsic limit in the resolution of a contact map. We used a threshold of 9 Å between C_α atoms to define contact; for this threshold the distance between two typical structures, that are both compatible with the contact map, is about 1 Å. The threshold of 9 Å is relevant for our purpose, of working with contact energies in a scheme to derive structure from sequence.

IV. DYNAMICS IN CONTACT MAP SPACE

We describe a stochastic method to perform dynamics in contact map space. We explain how the motion is restricted to physical regions of the space.

Our aim is to generate a large number of contact maps that can serve as candidates for the native structure. Such maps are necessary for protein folding by means of energy minimization, as well as in order to generate decoys needed to test properties of various energy functions. Hence the requirements from any procedure that generates such maps are

- The generated maps should be physical.

- The maps should be “protein-like”; for example they should have secondary structure elements
- The maps should have low values of the energy (defined in terms of the sequence and the contact map)
- Efficiency - in order to generate large numbers of independent maps in reasonable computing time.

The requirement of physicality is addressed by the method described in the Sec. III; whenever a new candidate map is generated, we use it as the target map of the reconstruction procedure, and obtain, this way, a contact map which corresponds to a physical “chain of beads”.

In order to move efficiently in contact map space in a way that satisfies the requirements listed above, we introduced a four-step procedure which is delined below. For further details we refer to Vendruscolo and Domany (1998a).

1. Non-Local Dynamics:

Starting from an existing map, we perform large scale “cluster” moves. Clusters are in approximate correspondence with secondary structure elements. At this stage, no attempt is made to preserve physicality. The contact map which is obtained by this procedure is typically uncorrelated to the starting one.

2. Local Dynamics:

The resulting map is refined by using local moves of different kinds. Secondary structure formation can be viewed as a “growth” process. Starting from a random coil, an α helix is formed by twisting one turn at a time (Chakrabartty and Baldwin, 1995). Analogously, an helix can translate locally by untwisting a turn at one extreme and reforming it at the opposite end, in a movement reminiscent to the reptation dynamics of polymers (de Gennes, 1979). A β sheet is created and removed by zipping and unzipping together two β strands (Muñoz *et al.*, 1997). We also use the conservative dynamics introduced by Mirny and Domany (1996) to further refine the resulting map.

3. Reconstruction:

We use the previously introduced reconstruction algorithm (Vendruscolo *et al.*, 1997) to restore physicality by projecting the map obtained from the second step onto the physical subspace.

4. Refinement:

We perform further optimization by energy minimization in *real space* using standard crankshaft moves (Šali *et al.*, 1994; Vendruscolo and Domany, 1998a).

The projection procedure from a contact map to its three dimensional counterpart is the bottleneck of the method. The dynamic rules that we introduce are aimed at generating uncorrelated starting points for this reconstruction. In this way, after each four-step move, we obtain a good candidate map for the native state. The contact energy (eq. 15) with some standard parametrization (i.e. choice of the $w(a,b)$) is used in steps 1, 2 and 4 following the standard Metropolis prescription for the acceptance of a move.

A. Non-local dynamics

Rules of non-local dynamics have been introduced in the context of the simulation of equilibrium properties of spin systems (Kandel and Domany, 1991) and of surfaces (Evertz *et al.*, 1991). Under suitable conditions, systems with a large number of degrees of freedom arrange themselves in conformations where the degrees of freedom are “coherently” grouped together. Using an incoherent dynamic procedure the time it takes to go from one coherent conformation to another can be prohibitively long. Physical intuition guides the choice of non-local rules to obtain an efficient dynamics. Since in our case we are developing a minimization algorithm, we are not concerned with detailed balance, and we can optimize the dynamics by choosing moves that minimize the energy.

We now present the physical considerations that guided our choice of non-local moves. The unknown interactions between amino acids dictate the rules that determine the stability of protein folds. Such rules

govern the chain topology in a rather stringent way. The overall number of existing protein families is estimated to be around 1000 (Chothia, 1992; Orengo *et al.*, 1994). Protein families are characterized by particular arrangements of secondary structures. Secondary structure elements are easily identified also in a contact map as clusters of points of characteristic size, shape and location. In the contact map representation, secondary structures can be handled very efficiently by binary operations. For example a parallel β sheet is created by turning from 0 to 1 a set of contacts forming a cluster with the shape of a thin band parallel to the main diagonal. To turn a 2- α bundle from an up-down topology to the alternative up-up one, a rotation of a cluster of points is required. The operations described provide only a scaffold, which is non physical, and must be rectified by the other two steps of the dynamics. The procedure yields every time a completely new topology. A MD simulation could obtain the same result only by completely (or at least partially) unfolding and refolding the protein.

In contact maps of experimentally determined protein structures clusters of contacts can be divided in four classes. Thick bands of adjacent contacts along the main diagonal represent α helices (see region 1 in Fig. 4a). Thin bands represent parallel β sheets if they are parallel to the main diagonal (region 2 in Fig. 4a) and antiparallel β sheets if they are antiparallel (region 3 in Fig. 4a). Small clusters or isolated points represent structurally relevant contacts between amino acids that are well separated along the sequence. These features characterize protein-like contact maps and should be preserved by the dynamics in contact map space.

As a preliminary information we determine the expected number N_c^* of contacts and the number N_s^* of clusters that are expected to appear in the contact map. These numbers will be stochastically conserved during the dynamics. We have already presented evidence to the effect (Vendruscolo *et al.*, 1997) that $N_c^* = aN^\nu$, where N is the length of the protein, $\nu \simeq 1$ and a depends on the threshold that is used to define a contact. As for N_s^* , there are algorithms to predict the secondary structure content, like the PHD (Rost and Sander, 1993) or the GOR (Garnier *et al.*, 1996) algorithms. Alternatively, having a good starting guess for the native contact map, one can directly determine N_c^* and N_s^* . The cluster algorithm is divided into three steps: labeling, deletion and creation.

1. *Labeling:*

Starting from an existing map, the first step is to identify the clusters that are present, which is done using the Hoshel-Kopelman algorithm (Stauffer and Aharony, 1992). With our definition of contact, contacts S_{ij} with $|i - j| \leq 2$ are always present due to chain connectivity, see Fig. 4a. Our dynamical rules do not violate these topological constraints. Cluster labeling is made in the upper triangle, excluding the first three diagonals. By symmetry, it is sufficient to perform all the dynamics in this region. At this stage we calculate the number N_c of contacts and the number N_s of secondary structures. Secondary structures are defined as cluster of more than $H = 10$ points. After this labeling procedure, each point (i, j) in the map has label $L(i, j) = (C, K)$ with a class C and a number K inside the class. Five classes are considered. In class α we put the clusters that are formed by bands along the main diagonal. In class β_{\parallel} we put the clusters that constitute bands parallel to the main diagonal but apart from it. In class β_{\perp} we group clusters that are in the form of bands perpendicular to the main diagonal. In the fourth class we gather all the remaining irregular clusters. In the last class we put all the points which do not belong to any cluster (e.g. isolated points).

2. *Destruction:*

N^- existing clusters are deleted from the map. N^- is chosen from a uniform random distribution between 1 and N_s . Destruction is simply realized by choosing at random a label (C, K) and by turning contacts in the corresponding cluster from 1 to 0.

3. *Creation:*

N^+ clusters are created in the map. N^+ is drawn from a gaussian distribution of mean $N_s^* - (N_s - N^-)$ and variance 1. If $N_s - N^- > N_s^*$ then $N^+ = 0$. Each time we make M attempts to create a cluster (typically $M = 100$), and we choose the one with the more favorable energy, according to Eq. (15). At each creation we first decide with probability $P(\alpha)$, $P(\beta_{\parallel})$ and $P(\beta_{\perp})$ whether to grow an α , a β_{\parallel} or a β_{\perp} . Typically $P(\alpha) = P(\beta_{\parallel}) = P(\beta_{\perp}) = 1/3$. The length of the created band is a uniform random number in $[5, 30]$ for α , in $[5, 12]$ for β_{\parallel} and β_{\perp} . Creation starts by selecting randomly a seed point

on the map. For α clusters this point is chosen on the principal diagonal, for β_{\parallel} at a point displaced from the principal diagonal by more than the length of the cluster. No restrictions are imposed on the seed of β_{\perp} . From this point we lay down a cluster in the form of a band as shown in Fig. 4b. We do not allow secondary structures to overlap or to be closer than 4 spacings on the map, since this is not commonly observed in actual contact maps. If while growing the cluster we encounter a point which already has a label that violates this condition we restart the creation. The result of a non-local move for 1ubq, starting from the native map shown in Fig. 4a is shown in Fig. 4b.

B. Local dynamics

The principal aim of these moves is to allow local rearrangements of the secondary structures that have been placed by the non-local dynamics. We first give the dynamical rules to deal with α helices. Consider an helix of n amino acids, which we have previously identified as starting from amino acid i and ending on $i+n$. Typically, n ranges from 5 to 30. To increase the size from the head, we add the two contacts $(i+n+1, i+n-2)$, $(i+n+1, i+n-3)$. The tail is increased by adding the two contacts above the diagonal $(i-1, i+2)$ and $(i-1, i+3)$. To decrease the size of the helix, one removes the contacts $(i+n, i+n-3)$ and $(i+n, i+n-4)$ on the head and $(i, i+3)$ and $(i, i+4)$ on the tail. To translate the helix, one performs a reptation-like move in which one turn is removed from one end and added to the other, by using the same rules.

Similar rules govern the growth and the translation of sheets. Consider first an antiparallel β sheet formed by two strands. The first strand extends from amino acids i to $i+n$ and the second from j to $j+m$. By unzipping amino acids $i+n$ and j , we reduce the size at the end closer to the main diagonal. This move is realized by setting to 0 (irrespective of their state) the five contacts $(i+n, j+2)$, $(i+n-1, j+2)$, $(i+n-1, j+1)$, $(i+n-2, j+1)$ and $(i+n-2, j)$. Opening the sheet from the other side is realized by setting to 0 the contacts $(i+2, j+m)$, $(i+2, j+m-1)$, $(i+1, j+m-1)$, $(i+1, j+m-2)$ and $(i, j+m-2)$. Zipping together the ends is realized by setting the corresponding contacts to one. Translating the sheets, as in the case of helices, is realized by opening one end while closing the other. Rules that are entirely similar are applied to parallel β sheets. In the general case, the sheet might present irregularities which would appear as supplementary contacts at the extremities. Since we do not attempt here to realize a physical map we implement these simple rules and rely on the reconstruction procedure to take care of the local structural details. The resulting contact map after this step is shown in Fig. 4c. We use the conservative dynamics introduced by Mirny and Domany (1996) to further refine the resulting map; the result is shown in Fig. 4d. Typically minor local rearrangements take place.

C. Reconstruction

As already observed, a generic contact map is not guaranteed to correspond to any real chain conformation in space. This is likely the case of the contact map obtained after the first two steps of the dynamics. By using the reconstruction method presented above we project this contact map onto its closest physical counterpart, i.e., we create a contact map which is “close” to the starting one, as measured by the Hamming distance, and is guaranteed to be physical, i.e., there is a real chain conformation which has that contact map. To achieve this result, we construct a backbone conformation in cartesian space and try to force it to have the contacts specified in the input contact map. If an input contact map is non-physical, existing contacts are discarded and possibly new ones are introduced. Since, however, any difference in the number and locations of contacts is penalized, the contact map of the resulting conformation is necessarily close to the starting one (Vendruscolo *et al.*, 1997). Monomers are not allowed to invade each other’s space. This is ensured by introducing a lower threshold R_L , below which they experience a hard-core repulsion. The lowest C_{α} - C_{α} distance found in PDB proteins is around 3.5 Å. We chose $R_L=5.0$ Å. With such a value, it is still possible to reconstruct all the PDB proteins and the tendency to create too compact structures, typical of the contact energy approximation, is minimized. Result of the reconstruction is shown in Fig. 4e.

D. Refinement:

We perform further optimization by an energy minimization in real space using a standard Metropolis crankshaft technique (Šali *et al.*, 1994; Vendruscolo and Domany, 1998a). Result of the minimization is shown in Fig. 4f. In this calculation we used a set \mathbf{w}_{153} of contact energy parameters, that was derived using the method presented by Mirny and Domany (1996), applied to the database of 153 proteins listed in Vendruscolo *et. al* (1998) with the present definition of contact. The initial energy of the native fold of 1ubq is 25.72 and the energy of the final map is much lower, -84.20.

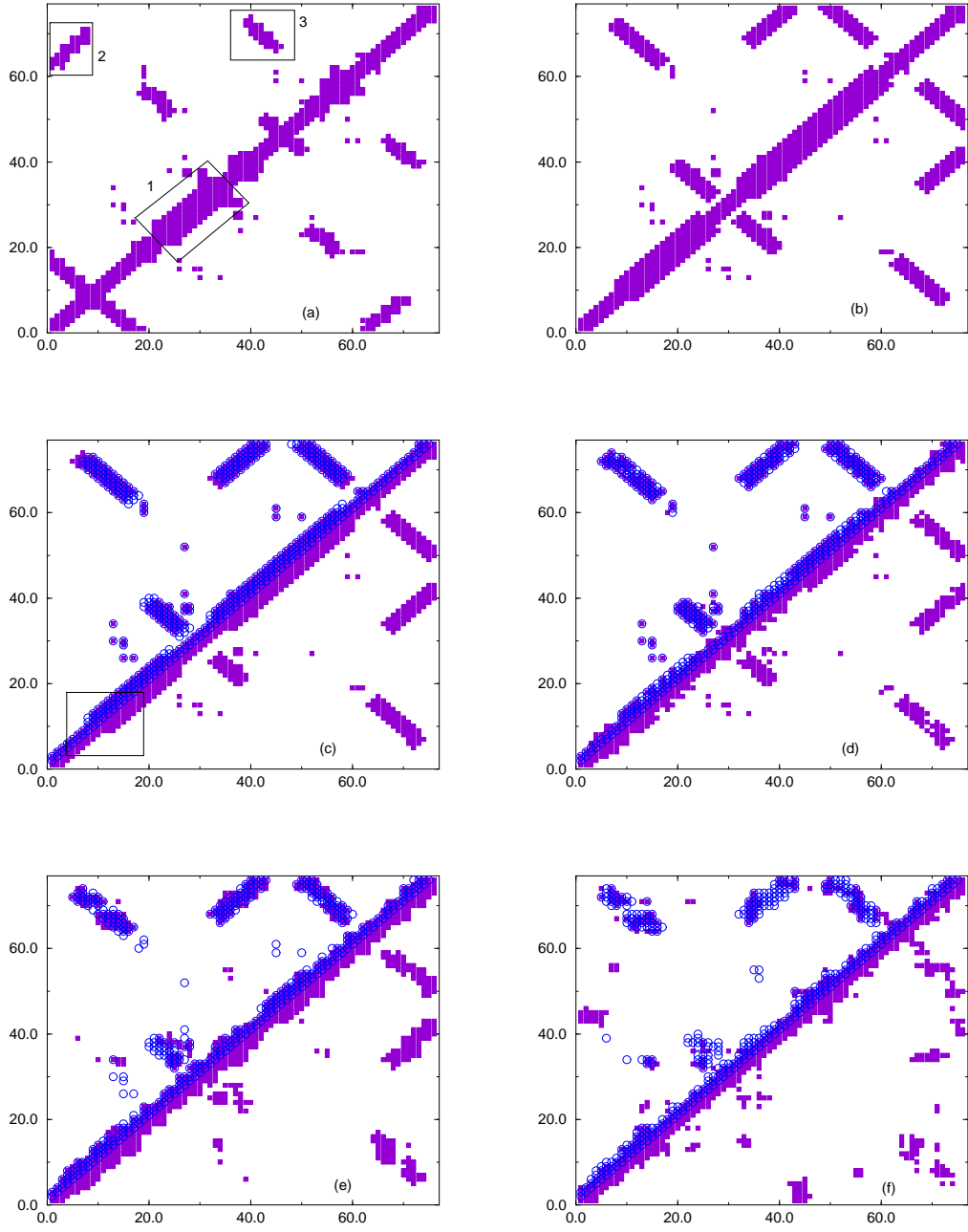


FIG. 4. (a) Contact map for the native state of protein ubiquitin (1ubq). There are 292 non-nearest neighbors contacts. Region 1 is an α helix, region 2 a parallel β sheet, and region 3 an antiparallel β sheet. (b) Contact map after a step of the non-local dynamics. (c) After a step of the local growth dynamics. The untwisting of a helix is shown in the box. (d) After a step of the local conservative dynamics. (e) After reconstruction. (f) After final minimization in real space. In (c-f) squares are the current map and circles the previous one. (Reprinted with permission from Vendruscolo and Domany (1998a). Copyright 1998 Current Biology.)

V. AN APPROXIMATION FOR THE FREE ENERGY

First, we introduce the exact free energy of a contact map and discuss two simple approximations to it. Second, we present a method to derive energy parameters based on perceptron learning.

A. The (free) energy associated with a contact map

As explained above, many microscopic configurations of a protein with sequence $\mathbf{A} = (a_1, a_2, a_3, \dots, a_N)$ are characterized by the same contact map \mathbf{S} . We now show that one can define an *exact free energy*, $\mathcal{H}(\mathbf{A}, \mathbf{S})$, for the assignment of \mathbf{S} to the sequence \mathbf{A} . Denote by \mathcal{C} a micro-state of the system, specified by the coordinates of all atoms of the protein (and of the solvent and any other relevant molecules). The true, microscopic energy of this configuration is $E(\mathcal{C})$. In thermal equilibrium each micro-state appears with a probability proportional to the corresponding Boltzmann weight $e^{-\frac{1}{kT}E(\mathcal{C})}$.

The *free energy* $\mathcal{H}(\mathbf{A}, \mathbf{S})$ (to which we refer simply energy) associated with sequence \mathbf{A} and map \mathbf{S} is defined as follows:

$$\text{Prob}(\mathbf{S}) \propto e^{-\mathcal{H}(\mathbf{A}, \mathbf{S})} = \sum_{\mathcal{C}} e^{-\frac{1}{kT}E(\mathcal{C})} \Delta(\mathcal{C}, \mathbf{S}) \quad (13)$$

where

$$\Delta(\mathcal{C}, \mathbf{S}) = \begin{cases} 1 & \text{if } \mathbf{S} \text{ consistent with } \mathcal{C} \\ 0 & \text{otherwise} \end{cases}$$

$\Delta(\mathcal{C}, \mathbf{S})$ is a “projection operator” that ensures that only those configurations \mathcal{C} whose contact map is \mathbf{S} contribute to the sum (13). In other words, only those micro-states whose contact map is \mathbf{S} contribute to the sum and hence to $\mathcal{H}(\mathbf{A}, \mathbf{S})$.

This definition of the (free) energy of a map is exact; it is nothing but the negative log of the *probability* of observing the map \mathbf{S} for sequence \mathbf{A} . Therefore $\mathcal{H}(\mathbf{A}, \mathbf{S})$ has an important property; inasmuch as the native fold’s contact map, \mathbf{S}_0 , has the highest probability of appearing the corresponding (free) energy, $\mathcal{H}(\mathbf{S}_0, \mathbf{A})$ is the *lowest* among all possible $\mathcal{H}(\mathbf{A}, \mathbf{S})$, i.e.

$$\mathcal{H}(\mathbf{A}, \mathbf{S}_0) < \mathcal{H}(\mathbf{A}, \mathbf{S}) \quad \forall \mathbf{S} \neq \mathbf{S}_0 \quad (14)$$

The main problem with this exact energy is that the sum (13) is impossible to carry out. Therefore, one takes various phenomenologically motivated guesses for the form of $\mathcal{H}(\mathbf{A}, \mathbf{S})$, that presumably would have been obtained had the sum been carried out. This approach is related in spirit to the phenomenological Landau-Ginzburg type free energy used in several areas of condensed matter physics. We also start from the simplest approximate form for this complicated function - that of the *pairwise contact energy*:

$$\mathcal{H}^{pair}(\mathbf{A}, \mathbf{S}) = \sum_{i < j}^N \mathbf{S}_{ij} w(a_i, a_j) \quad (15)$$

That is, if there is a contact between residues i and j , the parameter $w(a_i, a_j)$, which represents the energy gained by bringing amino acids a_i and a_j in contact is added to the energy.

Another term that has been introduced (Mirny and Domany, 1996) in the same spirit is a *hydrophobic*, (or solvation) term, of the form

$$\mathcal{H}^{hydro}(\mathbf{A}, \mathbf{S}) = \sum_i^N \left[\beta(a_i) \left(\sum_{k \neq i}^N \mathbf{S}_{ik} - n(a_i) \right)^2 \right] \quad (16)$$

Here $n(a)$ is the desired number of contacts that amino acid a should have - as obtained from the PDB, for example. A hydrophobic residue will have a larger value of n than a hydrophilic one. The term penalizes the configuration for deviations of the actual number of contacts of a_i , as read from the map \mathbf{S} , from the desired $n(a_i)$. Whereas the terms in \mathcal{H}^{pair} are specific to the residue with which a_i is in contact, here a_i does not “care” who are its partners. There may be some “double counting” in using both energy terms, but this should be compensated in the way one determines the parameters $w(a, b)$ and $\beta(a)$, the latter of which measure the strength of these hydrophobic terms. In our approach we determine the parameters by *learning*, with no recourse to a microscopic interpretation, so that we should not worry about double counting.

B. Optimization

In the energy function of the form of Eq. (15) one has to decide which set of parameters \mathbf{w} to use. The first idea was to derive a particular set of energy parameters from amino acid pairing frequencies observed in available crystallographic structures (Tanaka and Scheraga, 1976; Miyazawa and Jernigan, 1985).

An alternative method was proposed later by Maiorov and Crippen (1992). Energy parameters are derived by requiring that the observed native structures should be the lowest in energy among an ensemble of alternative conformations. Given the native contact map \mathbf{S}_0 , for each alternative map \mathbf{S} they wrote an inequality

$$\mathcal{H}^{pair}(\mathbf{A}, \mathbf{S}_0, \mathbf{w}) < \mathcal{H}^{pair}(\mathbf{A}, \mathbf{S}, \mathbf{w}), \quad (17)$$

and obtained the set \mathbf{w} from the solution of such inequalities. It was also realized that parameter derivation can be formulated as an optimization problem. For a fixed set of sequences with their native maps and for a fixed set of alternative contact maps, one defines a cost function in parameter space and looks for the set of parameters of “minimum cost”. Goldstein *et al.* (1992) maximized the ratio R between the width of the distribution of the energy and the average energy difference between the native state and the unfolded ones. More recently Mirny and Shakhnovich (1996) expressed the Z score as a function of the energy parameters which were then derived by optimization.

C. Learning the energy parameters by a perceptron

We set out to determine the energy parameters on the basis of the **basic requirement** (14). The basic requirement expresses the condition that the energy should attain its lowest value at the *true native map*. It can be stated by posing the following question:

Is it possible choose energy parameters such that for all the proteins in the database the native states have the lowest energy among all possible decoys?

We choose one protein (or more) with a known native map \mathbf{S}_0 and generate for it a large set of decoys \mathbf{S}_μ ; then we look for 210 contact parameters for which the inequalities (17) hold for all \mathbf{S}_μ .

The basic attribute of \mathcal{H}^{pair} that we use is its linearity in the contact energies $w(a, b)$; for any map \mathbf{S}_μ the energy (15) is a linear function of the 210 contact energies that can appear and it can be written as

$$\mathcal{H}^{pair}(\mathbf{A}, \mathbf{S}_\mu, \mathbf{w}) = \sum_{c=1}^{210} N_c(\mathbf{S}_\mu) w_c \quad (18)$$

Here the index $c = 1, 2, \dots, 210$ labels the different contacts that can appear and $N_c(\mathbf{S}_\mu)$ is the total number of contacts of type c that actually appear in map \mathbf{S}_μ . The difference between the energy of this map and the native one is therefore

$$\Delta \mathcal{H}_\mu^{pair} = \sum_{c=1}^{210} w_c x_c^\mu = \mathbf{w} \cdot \mathbf{x}_\mu \quad (19)$$

where we used the notation

$$x_c^\mu = N_c(\mathbf{S}_\mu) - N_c(\mathbf{S}_0) \quad (20)$$

and \mathbf{S}_0 is the native map.

Also the difference in the hydrophobic energy between the decoy \mathbf{S}_μ and the native map can be cast in a linear form. To see this, note that

$$\mathcal{H}^{hydro}(\mathbf{a}, \mathbf{S}_\mu, \mathbf{v}) = \sum_{c=1}^{20} M_c(\mathbf{S}_\mu) v_c . \quad (21)$$

In this case the index c runs over the 20 species of amino acids and

$$M_c(\mathbf{S}_\mu) = \sum_{i=1}^N \left[\sum_{k \neq i}^N \mathbf{S}_{ik, \mu} - n(a_c) \right]^2 \delta(a_i, c) , \quad (22)$$

where $\delta(a_i, c) = 1$ if $a_i = c$ and 0 otherwise.

The difference between the hydrophobic energy of this map and the native one is therefore

$$\Delta \mathcal{H}_\mu^{hydro} = \sum_{c=1}^{20} v_c y_c^\mu = \mathbf{v} \cdot \mathbf{y}_\mu \quad (23)$$

where we used the notation

$$y_c^\mu = M_c(\mathbf{S}_\mu) - M_c(\mathbf{S}_0) \quad (24)$$

In the presence of the hydrophobic term, the inequality (14) can then be written as

$$\Delta \mathcal{H}_\mu^{pair} + \Delta \mathcal{H}_\mu^{hydro} = \mathbf{w} \cdot \mathbf{x}_\mu + \mathbf{v} \cdot \mathbf{y}_\mu = \mathbf{u} \cdot \mathbf{z}_\mu > 0 , \quad (25)$$

where we introduced the following 230-components vectors

$$\begin{aligned} \mathbf{z} &= (x_1, \dots, x_{210}, y_1, \dots, y_{20}) \\ \mathbf{u} &= (w_1, \dots, w_{210}, v_1, \dots, v_{20}) . \end{aligned} \quad (26)$$

The total energy is linear in the parameters \mathbf{w} and \mathbf{v} .

We denote the normalization factor of the vector \mathbf{z}_μ by

$$Z_\mu = \sum_{c=1}^{230} (z_c^\mu)^2 , \quad (27)$$

and from here on we set $Z_c^\mu \leftarrow z_c^\mu / Z_\mu^{1/2}$, so that both \mathbf{z} and \mathbf{u} are normalized to 1.

Once the requirement (17), has been expressed using an energy in the form (25), the question whether it does or does not have a solution reduces to deciding whether a set of examples is learnable by a perceptron (Rosenblatt, 1962). Every candidate contact map provides a pattern for the training session.

The vector \mathbf{u} is “learned” in the course of a training session. The P patterns are presented cyclically; after presentation of pattern μ the weights \mathbf{u} are updated according to the following learning rule:

$$\mathbf{u}' = \begin{cases} (\mathbf{u} + \eta \mathbf{z}_\mu) / |\mathbf{u} + \eta \mathbf{z}_\mu| & \text{if } \mathbf{u} \cdot \mathbf{z}_\mu < 0 \\ \mathbf{u} & \text{otherwise} \end{cases} \quad (28)$$

This procedure is called learning since when the present \mathbf{u} misses the correct “answer” $h_\mu > 0$ for example μ , all weights are modified in a manner that reduces the error. No matter what initial guess for the \mathbf{u} one

takes, a convergence theorem guarantees that if a solution \mathbf{u} exists, it will be found in a finite number of training steps. Since the parameters \mathbf{v} have to be positive, we introduced the following trick. We added 20 fictitious examples \mathbf{z} which are vectors of zeros except the component $y_i, i = 1, \dots, 20$ which is set to 1.

Different choices are possible for the parameter η . Here we use the learning rule introduced by Nabutovsky and Domany (1991) since it allows, at least in principle, to assess whether the problem is learnable. The parameter η is given at each learning step by

$$\eta = \frac{-h_\mu + 1/d}{1 - h_\mu/d} \quad (29)$$

where the parameter d (called despair) evolves during learning according to

$$d' = \frac{d + \eta}{\sqrt{1 + 2\eta h_\mu + \eta^2}}. \quad (30)$$

Initially one sets $d = 1$.

The training session can terminate with only two possible outcomes. Either a solution is found (that is, no pattern that violates condition (25) is found in a cycle), or unlearnability is detected. The problem is *unlearnable* if the despair parameter d exceeds a critical threshold

$$d > d_c = \sqrt{M} [2Z_{max}]^{M/2}, \quad (31)$$

where M is the number of components of \mathbf{w} , and Z_{max} is the maximal value of the normalization factors (see Eq (27)). This value of d_c is easily derived for examples of the type of Eq (20), using the same method as given by Nabutovsky and Domany (1991).

It is easy to see that $\mathbf{u}^* = (\mathbf{w}^*, \mathbf{v}^*)$ is a solution of the system (25) if and only if $\mathbf{u}_\lambda^* = (\mathbf{w}^*, \lambda \mathbf{v}^*)$ is a solution of

$$\mathbf{w} \cdot \mathbf{x}_\mu + \frac{1}{\lambda} \mathbf{v} \cdot \mathbf{y}_\mu > 0. \quad (32)$$

The outcome of the learning process **does not** depend on the initial choice of λ . However, the learning time usually depends on λ which has to be chosen conveniently. A useful condition to set λ is to obtain on average $|\mathbf{x}| \sim |\mathbf{y}/\lambda|$.

VI. RESULTS

We prove in an extensive number of situations that the pairwise contact approximation both when alone and when supplemented with a hydrophobic term is unsuitable for stabilizing proteins' native states.

Whether or not the basic requirement (14) can be satisfied depends on several factors. We will discuss the dependence upon the following issues:

1. The definition of contact.
2. The assignment of the contact length R_c .
3. The number M_p of proteins in the database.
4. The method used to produce decoys.

A. Threading

We first discuss the dependence of learnability on M_p and R_c using the all atoms definition of contact and producing decoys by gapless threading. Once the contact maps of the M_p proteins in the database are obtained, decoys are generated for a given sequence of length N from the structures of proteins of lengths $N' (> N)$ by selecting submaps of size $N \times N$ along the main diagonal of the contact map of the longer protein. For each definition of contact that we considered we found two “phases”. There is a region in the (R_c, M_p) in which the problem is *learnable*; that is, there is a set \mathbf{w} of pairwise contact energy parameters that stabilize simultaneously all the native maps in the set. On the other hand, outside this region (e.g. for fixed R_c and large enough M_p) the problem is *unlearnable*, and no set \mathbf{w} exists.

Without doing any calculation, we can predict a few general features of the (R_c, M_p) phase diagram. Having set a definition of contact (e.g. the all atoms one) one can plot the distribution of distances between amino acid pairs. Choosing R_c smaller than the smallest observed distance would result in contact maps with no contacts, independently of the conformation. No set of energy parameters can then discriminate the native map from the decoys. Similarly, choosing R_c larger than the largest observed distance would result in contact maps with all the entries set to 1. In this case again no discrimination is possible. Thus we expect to find a window of learnability in R_c . It is also reasonable to expect that such a window will shrink with increasing M_p . The problem is thus reduced to investigate whether such window remains open for an arbitrary large value of M_p , or it closes for M_p large enough.

The boundaries of the region of learnability must be interpreted in a probabilistic sense. At given M_p and R_c , learnability depends on the particular choice of the proteins in the database. In principle one should define $P(R_c, M_p)$, the probability for a randomly extracted set to be learnable at (R_c, M_p) . The boundary is then defined by $P(R_c, M_p) = \text{const}$. In the present study, we chose not to give a precise numerical estimation of $P(R_c, M_p)$, which would require many extractions of sets of M_p proteins from the PDB and would be numerically intensive. We are interested in establishing the *existence* of the boundary rather than in its precise determination. Hence we will show that it is possible to find unlearnable datasets when their size is large enough.

The approximate boundaries of the region of learnability are shown in Fig. 5. The window of learnability shrinks to zero for M_p above 270. The precise value of the limit of learnability depends on the particular choice of proteins, and the fluctuations in M_p are of the order of few tens of proteins. Such fluctuations are larger than expected; they are due to a few proteins that are markedly more difficult to learn than others, and their inclusion in the dataset lowers the chances of learnability. For example 1vdfA and 1gotG are two such “hard to learn” proteins. 1vdfA is a chain of 46 amino acids which forms a single α helix; 1gotG is a chain formed by 2 α helices hinging at 90 degrees.

Each point shown in Fig. 5 is derived from a few (1 -3) randomly generated sets of M_p proteins in each. A full circle indicates that all the sets considered were learnable; open circles signal that at least one set was unlearnable. The largest fluctuations are found for small M_p at the right boundary. For example, for different sets with $M_p=20$ we found that the maximal R_c of learnability varies between 28 Å and 31 Å.

In this study, we selected five sets of protein structures from the PDB. The sets ranged from 154 to 945 proteins. The PDB is an archive of experimentally derived structures of proteins. To date, 8295 coordinate entries are deposited. It is known that the information contained in the entire PDB is redundant and some is incorrect. Routine methods are available to select subsets of non-homologous proteins whose experimental structures are determined reliably (Heringa *et al.*, 1992; Hobohm and Sander, 1994; Hooft *et al.* 1996).

Correlations between solutions at different M_p and R_c ranged from 0.22 (for a solution at $R_c = 7.5$ Å and $M_p = 200$ with a solution at $R_c = 4.5$ Å and $M_p = 154$) to 0.94, which is the typical correlation between two solutions of maximal stability at $R_c = 4.5$ Å and $M_p > 150$.

These findings indicate that with the all atoms definition of contact and the physically motivated choice of $R_c = 4.5$ Å (Mirny and Domany, 1996) it is possible to stabilize simultaneously, with high probability, about 200 randomly selected non homologous proteins against decoys generated by gapless threading.

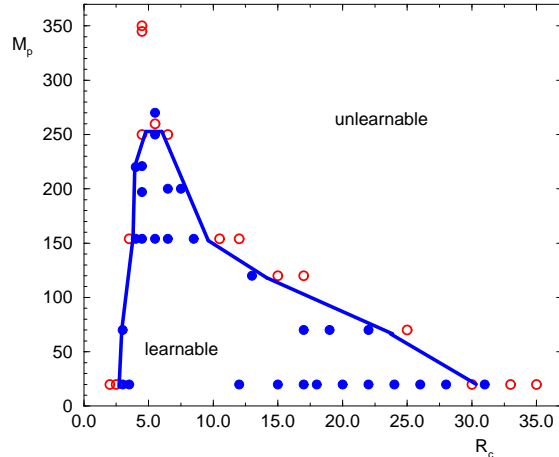


FIG. 5. Region of learnability for the all atoms definition of contact. Several sets of M_p proteins were generated for each value of R_c . Full circles indicate that all the sets considered for a particular value of (R_c, M_p) were learnable; otherwise we use open circles.

Which decoys are more challenging? It is instructive to consider the overlap Q between the contact map of the native state and of the decoys, which is defined as

$$Q = \frac{1}{\max(N_c^0, N_c^\mu)} \sum_{h>k+1}^N \mathbf{S}_{hk}^0 \mathbf{S}_{hk}^\mu, \quad (33)$$

where N is the length of protein and N_c^0 and N_c^μ are the number of contacts in \mathbf{S}^0 and \mathbf{S}^μ , respectively. We considered, for the C_α definition and $R_c=8.5 \text{ \AA}$, two sets of proteins. The first, of 123 proteins, is learnable and the second, of 141 proteins, unlearnable. First, for each decoy we calculated, using as initial weights the solution of an independent set of 197 proteins, the energy difference $\Delta\mathcal{H}$ with the native state and the overlap Q . In Figs. 6(a) and (b) we present scatter plots of $\Delta\mathcal{H}$ on Q for our decoys. The first question we asked is whether decoys of high overlap are the more challenging ones. To answer this question we repeated the learning procedure by considering only decoys with $Q < Q_t$, where Q_t is a threshold value for the overlap. The set of 141 proteins was still unlearnable for $Q_t = 0.6$. It seems that the “difficult” decoys are spread over the entire range of Q . Including all the decoys in the learning procedure we were able to learn the set of 123 proteins, but not the set of 141 proteins. As shown in Fig. 6(c), after learning the set of 123 proteins, decoys of low energy are present in the approximate range $0.2 < Q < 0.8$. The important finding is that the unlearnable case is not qualitatively different (see Fig. 6(d)). Also in this case decoys of low energy are present in the range $0.2 < Q < 0.8$, although now some of them have $\Delta\mathcal{H} < 0$. The difference is that with the set of 123 proteins there are 805,938 decoys, whereas for the set of 141 proteins, 1,071,753. With 210 energy parameters it is possible to satisfy the smaller set of inequalities but not the larger. Decoys of arbitrary Q enter in the learning process and one can argue that the lack of correlation between $\Delta\mathcal{H}$ and Q is a major cause that renders the problem unlearnable for large enough M_p and, further, that an improved energy function should first of all provide such a correlation.

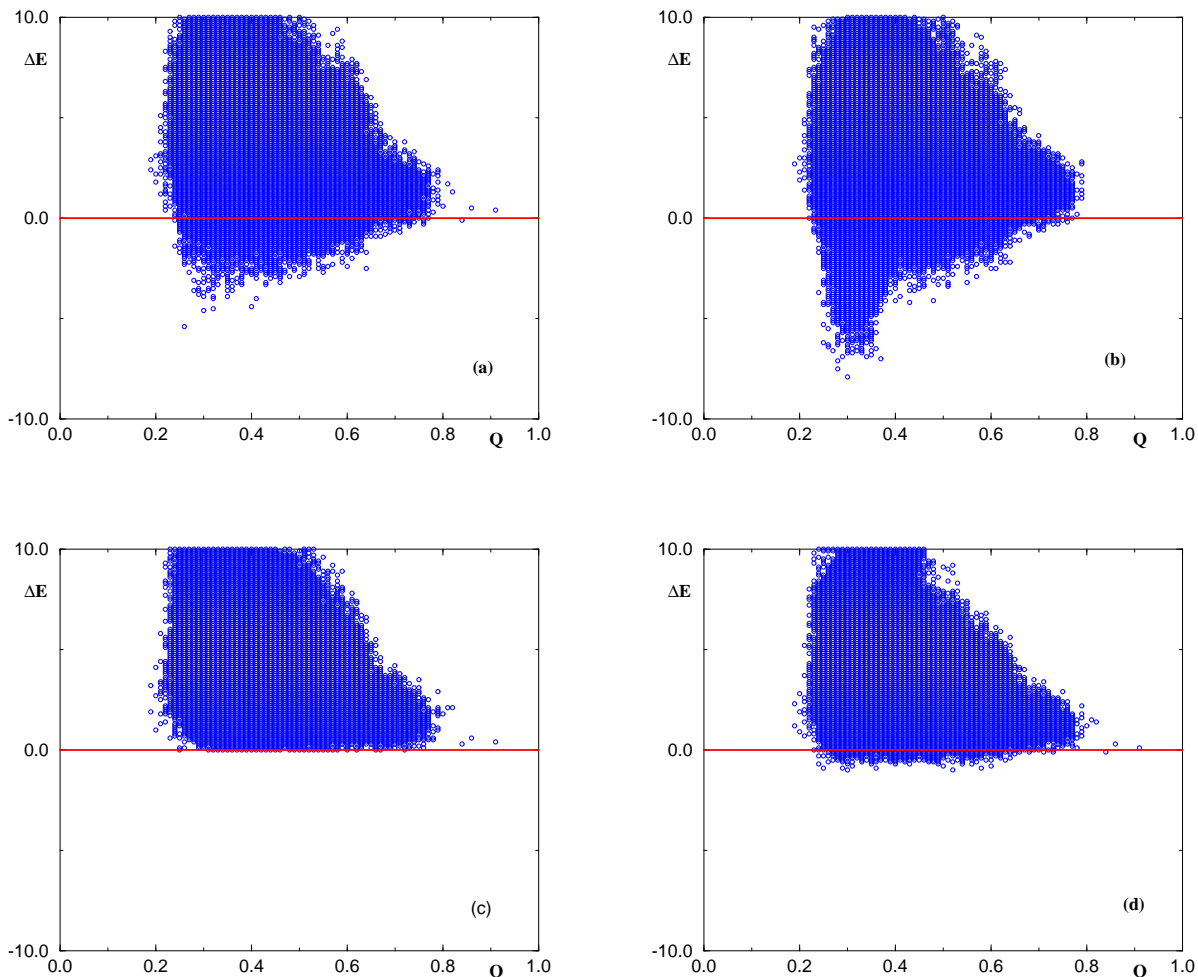


FIG. 6. Scatter plot of the energy difference \mathcal{H} between decoys and native state and the overlap Q with the native state, (a) Learnable set of 123 proteins for which the energy \mathcal{H}^{pair} was calculated using the solution of an independent set of 197 proteins; (b) Unlearnable set of 141 proteins with the same initial set of energy parameters; (c) The set of 123 proteins with the energy parameters obtained from learning; (d) The set of 141 proteins with the energy parameters arrived at when unlearnability has been established.

To investigate the dependence of learnability on the definition of contact we repeated the same analysis for two other definitions of contacts. The first based on C_α and the second on all carbon atoms – a contact was assumed if any two C atoms of the two amino acids were closer than R_c . In both cases we found regions of learnability qualitatively similar to the one shown in Fig. 5

To summarize, we showed that, no matter which definition of contact and which R_c are chosen, there is always a maximal number (of the order of few hundreds) of proteins that can be stabilized together. Is this number large or small? A definite answer is outside the limits of this study. It is *small* when compared with the total number of proteins existing in nature (hundreds of thousands), but it is fairly large when compared with the number of representative proteins in the PDB (also of the order of few hundreds (Hobohm and Sander, 1994)). We choose to generate decoys by gapless threading since it is a very efficient way to obtain decoys. To further generalize our conclusion, in the following sections we consider a more refined way to obtain decoys, based on energy minimization in the space of contact maps.

B. Crambin

The conclusion drawn from threading is that there is a maximal number of proteins that can be stabilized together using the pairwise contact approximation to the energy. One can ask a more limited question, namely if it is possible to fine tune energy parameters to stabilize just one protein, or possibly a set of proteins belonging to the same structural family. Threading offers poor contenders to the native state. Better candidates for the ground state are produced by contact map dynamics, the method presented in Sec. IV, which explores in an efficient way the space of contact maps. For a particular protein – crambin – we show in Fig. 7 that the decoys produced by threading are far less a challenge than those produced by contact map dynamics. The set of decoys obtained by threading can be learned – it is possible to produce a set of pairwise contact energy parameters that stabilizes crambin in a threading experiment. Here we ask the same question for decoys obtained by contact map dynamics (see point 4. at the beginning of this Section).

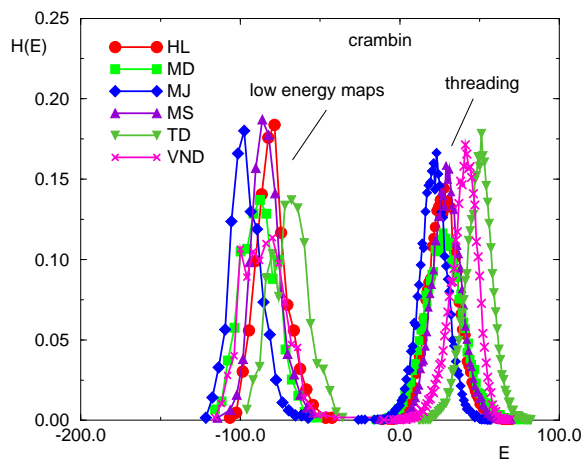


FIG. 7. Histograms that demonstrate the difference in energy between ensembles of contact maps obtained by threading and by energy minimization, shown for different contact energy parameters: (VND) as obtained in this work, by finding a solution for a threading ensemble; (HL): (Hinds and Levitt, 1994); (MD): (Mirny and Domany, 1996); (MJ): (Miyazawa and Jernigan, 1996); (MS): (Mirny and Shakhnovich, 1996); (TD): (Thomas and Dill, 1996). The energy parameter sets were shifted and rescaled to obtain $\langle \mathbf{w} \rangle = 0$ and $\langle \mathbf{w}^2 \rangle - \langle \mathbf{w} \rangle^2 = 1$ (averages are over the 210 energy parameters). Energies were shifted to set the native state to $E=0$.

Crambin (Teeter *et al.*, 1993) is a protein of length $N = 46$. We constructed its native map by taking the coordinates of the C_α atoms from the PDB and using a threshold of 8.5 \AA to define contacts. In the crambin chain, 5 out of the 20 amino acids do not appear and 3 appear only once. Thus, among the corresponding 210 possible contact energies, only 117 parameters can effectively enter the energy (15) for any set of candidate maps. These parameters form a 117-component vector \mathbf{w} . The native map contains 187 non-nearest neighbor contacts, which involve only 72 of the 117 possible contact energy parameters. We summarize here our main result about the question we have addressed in the present work. We will present below decisive evidence supporting our main conclusion:

the problem of fine tuning the pairwise contact energy parameters to stabilize the native state of crambin is *unsolvable*.

1. Learning the pairwise contact term

In an unlearnable case there exist sets of examples for which no solution can be found; for large enough P the training set will include, with non-vanishing probability, such an unlearnable subset.

The condition that has to be met (Nabutovsky and Domany, 1991) to establish unlearnability, is that the despair d , recorded during the learning process, should exceed the critical value d_c . According to Eq (31), for $M = 117$, we typically get a critical despair $d_c \simeq 10^{163}$.

In perceptron learning of $P > 2M$ randomly generated examples (which is an unlearnable problem (Cover, 1965; Gardner, 1988) for large M), d grows *exponentially* with learning time (Nabutovsky and Domany, 1991). Here, due to the specific non-random nature of the learning task, we need much more than $P = 2M = 234$ examples. Learning is realized in an iterative manner. Starting with an initial set of energy parameters we generate a set of examples that are then learned; the new set of energy parameters is used to generate new examples and so on. We will refer to each such iteration as an *epoch*. It was necessary to generate $P=298710$ examples in 11 epochs. We underscore the fact that each example was obtained by an energy minimization procedure, using the method discussed in Sec. IV. Learning this set of examples is an unsolvable task, proved by the divergence of the despair d . We reached $d > d_c$ after approximatively 37500 learning cycles. To speed up the procedure, without affecting the final result, we selected the 10000 examples at epoch 11 that had the lowest energy according to the energy parameters obtained from learning at epoch 10.

2. Energies of the false ground states

Even though the problem is unlearnable, our procedure produces contact energies that have several appealing features. The first is that whereas for the existing contact potentials it is very easy to find maps whose energy is below that of the native map, with the \mathbf{w} obtained after several training epochs this becomes a difficult (albeit possible) task. With the initial energy parameters the vast majority of the contact maps that are generated have a lower energy than the native contact map. As can be seen from Fig. 8, where the energy scale is shifted so that the native contact map has always zero energy, for increasing epoch index, the energy distribution shifts to the right and becomes narrower. Learning is thus accompanied by an improvement of the Z -score, which is a commonly used estimator of the quality of a set of energy parameters (Mirny and Shakhnovich, 1996). Hence our learning procedure flattens the energy landscape, reducing both the number of violating examples and their energy difference with the true native state. Another relevant question concerns the “location” of these false minima, i.e. how different are the corresponding structures from the native one? To study this, we reconstructed the three dimensional conformations corresponding to the violating examples and measured their average distance D (see Eq. 11) from the native conformation. We found that D does not decrease with the epoch index; moreover false minima are found at an approximate average D of 8 Å at *any* epoch. Only their number decreased significantly. Two compact uncorrelated conformations are typically found at a distance of 15 Å, which is also the result we obtained using other parameter sets taken from the literature.

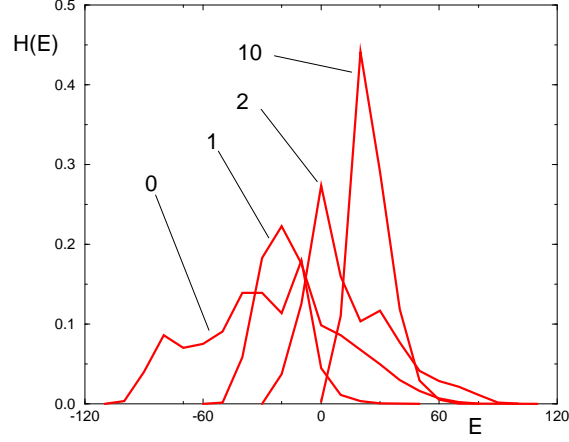


FIG. 8. Normalized histogram $H(\mathcal{H})$ of the energies of the contact maps at epochs $t = 0, 1, 2$ and 10. The energy scale is shifted so that the native contact map energy is 0. (Adapted with permission from Vendruscolo and Domany (1998b). Copyright 1998 American Institute of Physics.)

Here, we define the overlap Q between contact maps in a slightly different way as than in Eq. (33)

$$Q = \frac{N_p}{N_c} \quad (34)$$

where N_p is the number of contacts present in the native map *and* in the predicted one and N_c is the total number of contacts of the native map (contacts $(i, i + 1)$ and $(i, i + 2)$ are not counted). We generated 1000 low energy contact maps, using the set of energy parameters obtained at epoch 10. The histogram of the fraction of contact maps with a given overlap Q with the native state is shown in Fig. 5. The distribution is peaked at around 0.40, which means that typically we are able to correctly recover 40 % of the native contacts. We analyzed the distance D of the conformations corresponding to the maps of Fig. 9. We found that in the worst cases conformations are found at an approximate average D of 8 Å . It is not possible to improve this result, since the contact energy parameters cannot be optimized further.

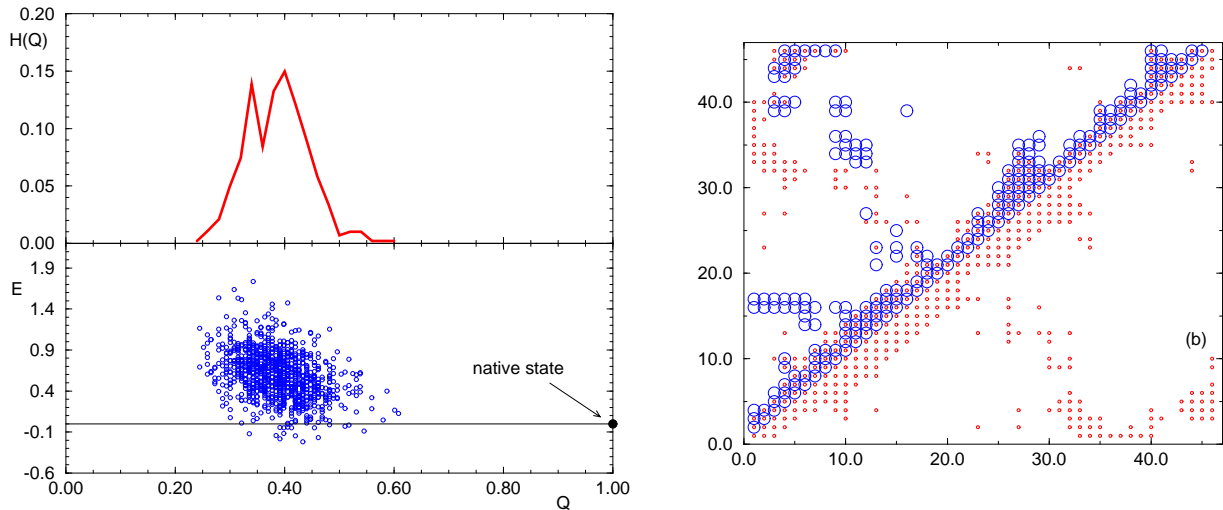


FIG. 9. (a) Result of the folding experiment on crambin described in the text in which we generated 1000 low energy decoys. Q is the fraction of correctly predicted contacts and \mathcal{H} is the energy difference between the decoy and the native state. (Adapted with permission from Vendruscolo and Domany (1998b). Copyright 1998 American Institute of Physics.) (b) Typical low energy map obtained during the simulation. Small dots indicate contacts in the native map, open circles contacts in the simulated map.

Consistently with our conclusion that the pairwise contact energy approximation is unsuitable for protein folding, Hao and Scheraga (1996) showed that a more accurate parametrization of the energy is capable of improving the performance in a folding simulation. They found that “when the crambin model is simulated to fold to the low-energy state with the optimized energy parameters, the folded structure is generally close to the target native structure”, although “the energy of the target structure was never able to separate completely from the continuous density of the nonnative states through the optimization”. They do find nonnative conformations with energy lower than the native state, but the contact maps of these have, on the average, high overlap with the native map.

One should not be misled by similar work on *model* proteins where, using a pairwise contact energy function, it is possible to discriminate the native state, either by optimization (Hao and Scheraga, 1996; Mirny and Shakhnovich, 1996; Hao and Scheraga, 1998) or by imposing conditions analogous to Eq (17) (Van Mourik *et al.*, 1998). In this case, a database of foldable sequences is designed using a pairwise contact potential and subsequently a set of contact energy parameters is recovered. Success in this case is possible because the contact energy of Eq (15) is the *exact* form of the free energy of the model.

3. Learning the hydrophobic term

We proved that the pairwise contact approximation is unsuitable to stabilize the native contact map of crambin against a set of decoys obtained by contact map dynamics. The next step we take is to improve it by adding the hydrophobic term (16) and ask again if the native state of crambin can be assigned with the lowest energy.

We found that the previously used set of 298710 decoys was learnable with the hydrophobic term. We increased the number of decoys to 390117 in 15 epochs and in this way we obtained an unlearnable set. After some trial we choose $\lambda = 15$ in eq. 32 since we found that the despair d grows faster for this choice.

Introducing the hydrophobic term does not make the problem learnable. However, it improves the situation depicted in Fig. 9. We repeated the folding experiment previously done (see Sec. VIB2). We found that the typical value of Q is larger, as shown in Fig. 10a. The average value of Q moves from 0.4 (pairwise term only) to 0.5 (hydrophobic term). These two values should be compared with 0.2, which is the value obtained for decoys produced by threading crambin into a set of 456 proteins (the distribution is marked by a T in the figure).

C. Immunoglobulins

Crambin could be a peculiar case since it is a short protein, it has only 15 species of amino acids, etc. To what extent the results about unlearnability extends to other proteins? To answer to this question we undertook a study of a set of proteins of the family of immunoglobulins.

An immunoglobulin molecule is formed by two light chains and two heavy ones (Branden and Tooze, 1991) held together by disulfide bridges and by the packing of their respective domains. The light chain folds into two domains, the variable V_L and the constant C_L and the heavy chain folds into four domain, one variable V_H and three constant C_{H1} , C_{H2} and C_{H3} . Sequence similarity in constant domains is typically above 35 % and around 10 to 20 % in variable domains.

We focused our study on the variable domains of the light chain V_L which is formed by two β -sheets, one of four strands and the other of six strands. The reason to choose immunoglobulins is mainly due to the extremely rich amount of information available. The sequence database of Kabat *et al.* (1991) now contains about 5700 different variable domains and the structure of about 140 are available from the PDB.

We asked the question if it is possible to stabilize 6 V_L domains simultaneously. The domains chosen were 8fab A, 1baf L, 1cbv L, 1dba L, 2f19 L and 1fdl L, whose respective lengths were 104, 107, 112, 107, 107 and 107 amino acids.

1. Learning the pairwise contact term

As opposed to the case of crambin, where only 117 pairwise contact species are present, all the 210 possible ones are present for immunoglobulins. To prove unlearnability, we adopted the same iterative procedure used for crambin. We generated 97309 examples, in 6 epochs. To speed up the procedure we considered only a subset of decoys, selected according to the following procedure. Consider the component c of the vector \mathbf{x}^μ of a particular decoy μ . If the numbers $N_c(S_\mu)$ and $N_c(S_0)$ are equal then $x_c^\mu = 0$ and this particular decoy can never be used to update w_c . If we initialize $w_c = 0$ and use only decoys with $x_c = 0$ then $w_c = 0$ during the entire learning procedure. We excluded all the decoys having contacts of 13 species, in this way we remained with 35677 decoys with 197 contact species. Obviously, for such a subset, adding the 13 energy parameters cannot change the result, since they never enter in the calculation of the energy. We further selected the 5000 decoys of lowest energy (according to the energy parameters learned at epoch 5) and performed the learning on this subset. In this way the critical value of the despair was surpassed in an amenable computer time.

2. Learning the hydrophobic term

The set of 97309 decoys was learnable by adding the hydrophobic term. We enlarged it to 110576. Using the same trick explained above, we excluded from the learning 13 pairwise contact energy terms. This selection procedure identified a subset of 42798 decoys for which we proved unlearnability.

The failure to assign the lowest energy to the native contact map is more severe in the case of immunoglobulins. The low energy contact maps in the case of crambin did resemble the native map to some extent, as shown in Fig. 9. In the case of immunoglobulins there is very little similarity between low energy maps and the native one (see Fig. 10b).

We think that this result deserves an explanation, which we propose in the following argument. As already done for crambin, we obtained a set of decoys by threading for immunoglobulins. Such a distribution is narrower and shifted to the left with respect to the corresponding distribution for crambin. We assume that threading offers random protein-like conformations. Therefore, the shift is originated by the exponential increase of the number of physical contact maps (Vendruscolo *et al.*, 1999) with the length of the proteins. The improvement, as measured by the right-shift of the distribution of Q , obtained by learning energy parameters, is comparable for crambin and for immunoglobulins. However, since immunoglobulins are longer, one would have to work harder to obtain energy parameters suitable for folding – many more decoys are to be weeded out. Since we proved that it is impossible to tune better the energy parameters for both approximations of the energy that we discussed, the only choice is to develop better forms for the energy. This will be the object of future study.

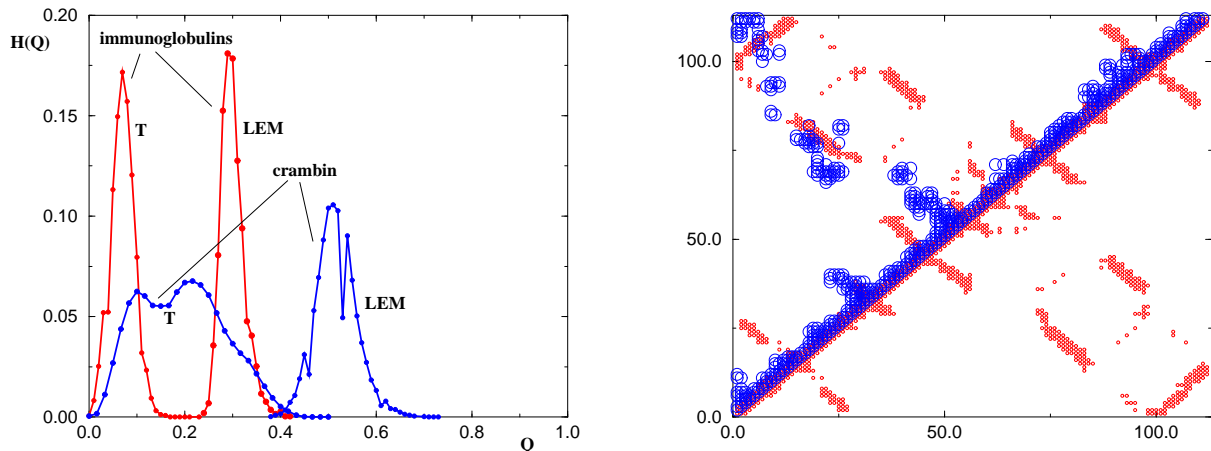


FIG. 10. (a) Histogram of the distribution of the overlap Q between maps of low energy (LEM) and the native map found in the simulation with the hydrophobic term for immunoglobulins and for crambin. For comparison, the distributions obtained by threading are also shown (T). (b) Typical low energy contact map (open circles) generated during the simulation of 1dba. For comparison the native map is also shown (full dots).

VII. FINAL CONSIDERATIONS

We presented the results of our attempt to perform protein folding in the space of contact maps.

- We demonstrated the feasibility of the original idea of performing energy minimization in contact map space.
- We proved that two simple phenomenological approximations to the free energy can not possibly be tuned to assign the lowest energy to the observed native conformation of even one single protein.
- We leave open the possibility to use better approximations for the free energy and more detailed representations of the chain underlying a contact map.
- We also leave open the possibility of predicting native states by other methodologies that do not use energy minimization.

ACKNOWLEDGMENTS

We are grateful to Ron Elber for discussing with us a similar approach, based on Eq. 14 (unpublished), and to Gaddy Getz, Ido Kanter, Edo Kussell, Rafael Najmanovich and Kibeom Park for their contributions to different parts of the work presented. This research was supported by grants from the Minerva Foundation, the Germany-Israel Science Foundation (GIF) and by a grant from the Israeli Ministry of Science.

[1] Anfinsen, C. (1973). Principles that govern the folding of protein chains. *Science* **181**, 223-230.

- [2] Aszodi, A., and Taylor, W. R. (1996). Homology modelling by distance geometry. *Fold. Des.* **1**, 325-334.
- [3] Bernstein, F. C., Koetzle, T. F., Williams, G. J. B., Meyer, E. F. Jr., Brice, M. D., Rodgers, J. R., Kennard, O., Shimanouchi, T., and Tasumi, M. (1977). The protein data bank: a computer-based archival file for macromolecular structures. *J. Mol. Biol.* **112**, 535-542.
- [4] Bohr, J., Bohr, H., Brunak, S., Cotterill, R. M., Fredholm, H., Lautrup, B., and Petersen, E. F. (1993). Protein structures from distance inequalities. *J. Mol. Biol.* **231**, 861-869.
- [5] Bowie, J. U., Luthy, R., and Eisenberg, D. (1992). A method to identify protein sequences that fold into a known 3-dimensional structure. *Science* **253**, 164-170.
- [6] Branden, C., and Tooze, J. (1991). Introduction to protein structure. Garland publishing, Inc. New York and London (1991).
- [7] Brooks, C. L. (1998). Simulation of protein folding and unfolding. *Curr. Op. Struct. Biol.* **8**, 222-226.
- [8] Brünger, A. T., Adams, P. D., and Rice, L. M. (1997). New applications of simulated annealing in X-rays crystallography and solution NMR. *Curr. Op. Struct. Biol.* **5**, 325-336.
- [9] Brünger, A. T., Clore, G. M., Gronenborn, A. M., and Karplus, M. (1986). Three-dimensional structure of proteins determined by molecular dynamics with interproton distance restraints: application to crambin. *Proc. Natl. Acad. Sci. USA* **83**, 3801-3805.
- [10] Chakrabartty, A., and Baldwin, R. L. (1995). α -helix stability. *Adv. Prot. Chem.* **46**, 141-176.
- [11] Chan, H. S., and Dill, K. A. (1990). Origins of structure in globular proteins. *Proc. Natl. Acad. Sci. USA* **87**, 6388-6392.
- [12] Chothia, C. (1992). One thousand families for the molecular biologist. *Nature* **357**, 543-544.
- [13] Clementi, C., Maritan, A., and Banavar, J. R. (1998). Folding, design, and determination of interaction potentials using off-lattice dynamics of model heteropolymers. *Phys. Rev. Lett.* **81**, 3287-3290.
- [14] Cover, T. (1965). Geometrical and statistical properties of systems of linear inequalities with applications in pattern recognition. *IEEE Trans. Elect. Comput.* **14**, 326.
- [15] Crippen, G., and Havel, T. F. (1988). Distance geometry and molecular conformation. Wiley, New York.
- [16] de Gennes, P. G., (1979). Scaling concepts in polymer physics. Cornell University Press, Ithaca NY.
- [17] Dinner, A. R., Šali, A., and Karplus, M. (1996). The folding mechanism of larger model proteins: the role of native structure. *Proc. Natl. Acad. Sci. USA* **93**, 8356 (1996).
- [18] Duan, Y., and Kollman, P. A. (1998). Pathways to a protein folding intermediate observed in a 1-microsecond simulation in water solution. *Science* **282**, 740-744.
- [19] Evertz, H. G., Hasenbush, M., Marcu, M., Pinn, K., and Solomon, S. (1991). High precision measurement of the SOS surface thickness in the rough phase. *J. de Physique I (France)* **1**, 1669-1674.
- [20] Fisher, D., Rice, D., Bowie, J. U., and Eisenberg, D. (1996). Assigning amino acid sequences to 3-dimensional protein folds. *FASEB J.* **10**, 126-136.
- [21] Gardner, E. (1988). The space of interactions in neural networks models. *J. Phys. A* **21**, 257.
- [22] Garnier, J., Gibrat, J. F., and Robson, B. (1996). GOR method for predicting protein secondary structure from amino acid sequence. *Meth. Enzymol.* **266**, 540-553.
- [23] Godzik, A., Skolnik, J., and Kolinski, A. (1993). Regularities in interaction patterns of globular proteins. *Protein Eng.* **6**, 801-810.
- [24] Goldstein, R., Luthey-Schulten, Z. A., and Wolynes, P. G. (1992). Optimal protein folding codes from spin glass theory. *Proc. Natl. Acad. Sci. USA* **89**, 4918-4922.
- [25] Hinds, D. A., and Levitt, M. (1994). Exploring conformational space with a simple lattice model for protein structure. *J. Mol. Biol.* **243**, 668-682.
- [26] Hao, M.-H., and Scheraga, H. A. (1996). How optimization of potential function affects protein folding. *Proc. Natl. Acad. Sci. USA* **93**, 4984-4989.
- [27] Hao, M.-H., and Scheraga, H. A. (1998). Molecular mechanisms for cooperative folding of proteins. *J. Mol. Biol.* **277**, 973-983.
- [28] Havel, T. F., Crippen, G. M., and Kuntz, I. D. (1979). Effect of distance constraints on macromolecular conformation. II. Simulation of experimental results and theoretical predictions. *Biopolymers* **18**, 73-81.
- [29] Havel, T. F., and Wüthrich, K. (1985). An evaluation of the combined use of nuclear magnetic resonance and distance geometry for the determination of protein conformation in solution. *J. Mol. Biol.* **182**, 281-294.
- [30] Heringa, J., Sommerfeldt, H., Higgins, D., and Argos, P. (1992). OBSTRUCT: A program to obtain largest cliques from a protein sequence set according to structural resolution and sequence similarity. *CABIOS* **8**, 599-600.
- [31] Hobohm, U., and Sander, C. (1994). Enlarged representative set of protein structure. *Protein Sci.* **3**, 522-524.
- [32] Holm, L., and Sander, C. (1993). Protein structure comparison by alignment of distance matrices. *J. Mol. Biol.*

233, 123-138.

- [33] Hooft, R. W., Vriend, G. Sander, C., and Abola, E. E. (1996). Errors in Protein Structures. *Nature* **381**, 272.
- [34] Irbäck A., and Potthast, F. (1995). Studies of off-lattice model for protein folding: sequence dependence and improved sampling at finite temperature. *J. Chem. Phys.* **103**, 10298-10305.
- [35] Jones, D. T., Taylor, W. R., and Thornton, J. M. (1992). A new approach to protein fold recognition. *Nature* **358**, 86-89.
- [36] Kabat, E., Wu, T., Perry, H., Gottesman, K., and Foeller, C. (1991). Sequences of proteins of immunological interest. NIH Publ. No 91-3242, 5th edit. DHHS, PHS, NIH, Bethesda, MD.
- [37] Kandel, D., and Domany, E. (1991) General cluster Monte Carlo dynamics, *Phys. Rev. B* **43**, 8539-8555.
- [38] Kirkpatrick, S., Gelatt, C. D. Jr, and Vecchi, M. P. (1983). Optimization by simulated annealing. *Science* **220**, 671-680.
- [39] Lifson, S., and Sander, C. (1979). Antiparallel and parallel beta-strands differ in amino acid residue preferences. *Nature* **282**, 109-111.
- [40] Lund, O., Hansen, J., Brunak, S., and Bohr, J. (1996). Relationship between protein structure and geometrical constraints. *Protein Science* **5**, 2217-2225.
- [41] Maiorov, V. N., and Crippen, G. M. (1992). Contact potential that recognizes the correct folding of globular proteins. *J. Mol. Biol.* **227**, 876-888.
- [42] McLachlan, A. D. (1979). Gene duplications in the structural evolution of chymotrypsin. *J. Mol. Biol.* **128**, 49-79.
- [43] Mirny, L., and Domany, E. (1996). Protein fold recognition and dynamics in the space of contact maps. *Proteins* **26**, 391-410.
- [44] Mirny, L., and Shakhnovich, E. I. (1996) How to derive a protein folding potential ? A new approach to an old problem. *J. Mol. Biol.* **264**, 1164-1179.
- [45] Miyazawa, S., and Jernigan, R. L. (1985). Estimation of effective interresidue contact energies from protein crystal structures: quasi-chemical approximation. *Macromolecules* **18**, 534-552.
- [46] Miyazawa, S., and Jernigan, R. L. (1996). Residue-residue potentials with a favorable contact pair term and an unfavorable high packing density term, for simulation and threading. *J. Mol. Biol.* **256**, 623-644.
- [47] Mumenthaler, C., and Braun, W. (1996). Automated assignment of simulated and experimental NOESY spectra of proteins by feedback filtering and self-correcting distance geometry. *J. Mol. Biol.* **254**, 465-480.
- [48] Muñoz, V., Thompson, P. A., Hofrichter, J., and Eaton, W. A. (1997). Folding dynamics and mechanism of β -hairpin formation. *Nature* **390**, 196-199.
- [49] Nabutovsky, D., and Domany, E. (1991). Learning the unlearnable. *Neural Computation* **3**, 604
- [50] Nilges, M. (1995). Calculation of protein structure with ambiguous distance restraints. Automated assignment of ambiguous NOE crosspeaks and disulfide connectivities. *J. Mol. Biol.* **245**, 645-660.
- [51] Novotny, J., Brucoleri, R., and Karplus, M. (1984). An analysis of incorrectly folded protein models. Implications for structure prediction. *J. Mol. Biol.* **177**, 787-818.
- [52] Olmea, O., and Valencia, A. (1997). Improving contact predictions by the combination of correlated mutations and other sources of sequence information. *Fold. Des.* **2**, S25-S32.
- [53] Orengo, C. A., Jones, D. T., and Thornton, J. M. (1994). Protein superfamilies and domain superfolds. *Nature* **372** 631-634.
- [54] Ortiz, A. R., Kolinski, A., and Skolnick, J. (1998). Nativelike topology assembly of small proteins using predicted restraints in Monte Carlo simulations. *Proc. Natl. Acad. Sci. USA* **95**, 1020 (1998).
- [55] Park, B. H., and Levitt, M. (1995). Energy functions that discriminate x-ray and near-native folds from well-constructed decoys. *J. Mol. Biol.* **249**, 493 (1995).
- [56] Rosenblatt, F. (1962). Principles of neurodynamics. Spartan books, New York.
- [57] Rosenbluth, M. N., and Rosenbluth, A. W. (1955). Monte Carlo calculation of the average extension of molecular chains. *J. Chem. Phys.* **23**, 356-359.
- [58] Rost, B., and Sander, C. (1993). Improved prediction of protein secondary structure by use of sequence profile and neural networks. *Proc. Natl. Acad. Sci. USA* **90**, 7558-7562.
- [59] Šali, A., Shakhnovich, E. I., and Karplus, M. (1994). Kinetics of protein folding. A lattice model study of the requirements for folding to the native state. *J. Mol. Biol.* **235**, 1614-1636.
- [60] Scheek, R. M., van Gunsteren, W. F., and Kaptein, R. (1989). Molecular Dynamics simulation techniques for determination of molecular structures from nuclear magnetic resonance data. *Methods Enzymol.* **177**, 204-218.
- [61] Skolnick, J., Kolinski, A., and Ortiz, A. R. (1997). MONSSTER: A method for folding globular proteins with a small number of distance restraints. *J. Mol. Biol.* **265**, 217-241.

- [62] Stauffer, D., and Aharony, A. (1992). *Introduction to percolation theory*. Second Edition, Taylor & Francis Eds., London.
- [63] Tanaka, S., and Scheraga, H. A. (1976). Medium- and long-range interaction parameters between amino acids for predicting three-dimensional structures of proteins. *Macromolecules* **9**, 945-950.
- [64] Teeter, M. M., Roe, S. M., and Heo, N. H. (1993). Atomic resolution (0.83 Angstroms) crystal structure of the hydrophobic crambin at 130 K. *J. Mol. Biol.* **230**, 292-311.
- [65] Thomas, P. D., and Dill, K. A. (1996b). An iterative method for extracting energy-like quantities from protein structures. *Proc. Natl. Acad. Sci. USA* **93**, 11628-11633.
- [66] Van Mourik, J., Clementi, C., Maritan, A., Seno, F., and Banavar, J. R. (1998). Determination of interaction potentials of amino acids from native protein structures: test on simple lattice models. E-print cond-mat/9801137;
- [67] Vendruscolo, M., and Domany, E. (1998a). Efficient dynamics in the space of contact maps. *Fold. Des.* **3**, 329-336.
- [68] Vendruscolo, M., and Domany, E. (1998b). Pairwise contact potentials are unsuitable for protein folding *J. Chem. Phys.* **109**, 11101-11108.
- [69] Vendruscolo, M., Kussell, E., and Domany, E. (1997). Recovery of protein structure from contact maps. *Fold. Des.* **2**, 295-306.
- [70] Vendruscolo, M., Najmanovich, R., and Domany, E. (1998) A novel method to derive contact energy parameters from large databases obtained by threading *Protein Sci.*, submitted.
- [71] Vendruscolo, M., Subramanian, B., Kanter, I., Domany, E., and Lebowitz, J. L. (1999) Statistical properties of contact maps. *Phys. Rev. E*, **59**, 977-984 (1999).